

ATOMIC FORCE MICROSCOPY AND SOLID-STATE REARRANGEMENT OF BENZOPINACOL

GERD KAUPP* AND MICHAEL HAAK

FB 9–Organic Chemistry I, University of Oldenburg, D-26111 Oldenburg, Germany

AND

FUMIO TODA

Department of Applied Chemistry, Ehime University, Matsuyama, Ehime 790, Japan

The solid–solid chemical reaction of benzopinacol (1) with *p*-toluenesulphonic acid monohydrate (2) to give a quantitatively proton-catalysed pinacol rearrangement with formation of triphenylacetophenone (3) in the absence of a solvent was studied preparatively and mechanistically using atomic force microscopy (AFM) measurements and known crystal structure data. The reaction rate is dramatically enhanced if the water of reaction is continuously removed. AFM reveals that no reaction occurs on (001) of 1 whereas (100) exhibits distance dependent craters and volcano-like mounds over areas extending to 1.5 mm from the contact edge of the crystals with 1 undergoing phase rebuilding while reacting. A mechanism resembling the formation of membrane potentials is seen for the first time in crystals. Thus it appears that catalytic protons migrate without their counterions from one molecular compartment to the next by proton consumption at its inside and proton liberation at its outside, which is the inside of the next compartment. The uppermost molecular layer determines reactivity or non-reactivity. On (001) of 1 the hydroxyl groups occur with their hydrogens up. Hence no AFM features are found and crystals of 2 do not become adhered to 1. However, on (100) the hydroxyl hydrogens point down (free electron pair up). Protonation is possible, chemical reaction is indicated by the formation of the AFM features and crystals of 2 adhere firmly to the surface of 1 after reaction.

INTRODUCTION

Solid–solid reactions are unusual. New solids form just by mixing of ground reactive solids (sometimes with moderate heating) and the yields are usually high. In genuine cases there are no intervening liquid or gaseous phases. Numerous organic reactions of this type have been found recently,¹ but almost nothing is known about their mechanisms. The recent success in elucidations of gas–solid reaction mechanisms with atomic force microscopy (AFM) measurements² prompted investigations of solid–solid reactions using this technique. We report here on our basic findings with a new example of acid-catalysed solid–solid pinacol rearrangement (further examples are given in Reference 3). The data provide numerous hints for future developments of related synthetic techniques of the new generation which largely avoid waste formation in any form.

* Author for correspondence.

RESULTS AND DISCUSSION

In crystal–crystal reactions any anisotropies of molecular transports are most convincingly detected by AFM measurements if the area of solid–solid contact is well delineated and defined with respect to the crystallographic face of the reactant under consideration. Thus, even more detailed mechanistic answers are possible than in the field of gas–solid reactions.

If a tiny crystal of *p*-toluenesulphonic acid monohydrate (2) is laid down on the most prominent (001) surface of a single crystal of benzopinacol (1), that face can be conveniently probed with the 4 μm wide AFM tip next to the solid proton source closer than 0.1 mm or further apart. In this instance no change in surface features could be detected with the AFM within less than 1 nm height for reaction times of up to 3 days at room temperature or 12 h at 50 °C. However, if the (100) face was probed correspondingly, the distance-dependent features in Figure 1 were obtained reproducibly after heating at 50 °C for 12 h. With shorter

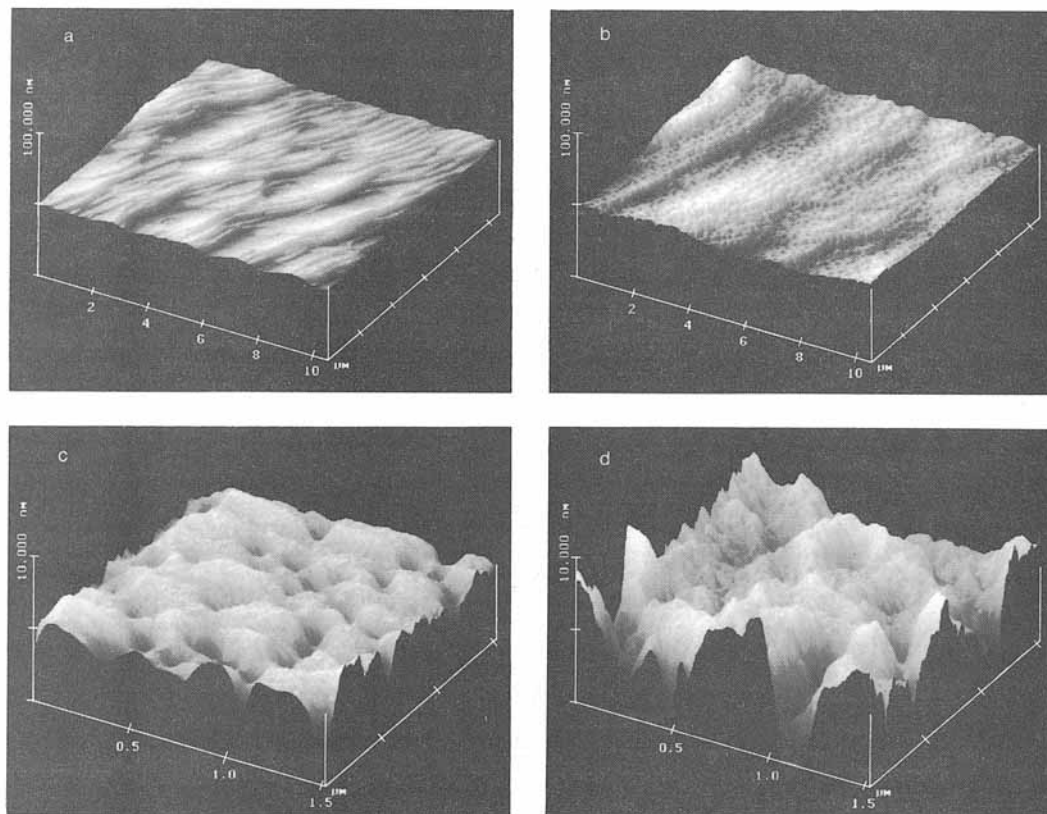


Figure 1. AFM surfaces of **1** on (100) showing distance-dependent phase rebuilding in its solid–solid pinacol rearrangement: (a) ca 0.5 mm beside a tiny crystal of **2** shortly after placing it; (b) and (c) at 0.5 mm distance and (d) at 0.1 mm distance after 12 h of reaction at 50.0 °C

reaction times (e.g. 2 h), features similar to those in Figure 1(c) were detected close to the solid proton source **2**. Surprisingly, no lateral anisotropic behaviour was found on the reactive face (100). The features along the crystallographic *b*-axis were also detected in directions of about 90°, 60° or 45° with respect to the *b*-axis from the onlying crystal of **2**, although it is hard to say if the spread of reaction was perfectly concentric or slightly elliptic. It can be seen in Figure 1(b) that the gross terrace structure in Figure 1(a) is retained at large distances. Apparently only a few molecular layers have reacted. The stability of the pictures even after ten and more AFM scans proves that no liquid is formed on the surface.^{2,4} The features are clearly distance dependent (Figure 1). The 1.5 μm scans show the situation at 0.5 mm [Figure 1(c)] and at 0.1 mm from the edge of the crystal **2** [Figure 1(d)]. The craters are regularly shaped with depths of up to 5 nm (slope 5°) and widths of 150 nm and some upward transport of solid material at 0.5 mm is seen. However, very close to the solid–solid contact edge, the original surface has completely

changed. At 0.1 mm the craters are 11 nm deep (slope 7°) and walls and volcano-like mounds of considerable height (e.g. 4 nm) have formed. Thus, considerable molecular transport has occurred perpendicular to (100). Interestingly, the lateral spread of reaction is much more efficient than the vertical spread. At a distance of 1 mm, smaller craters of roughly the same frequency as at 0.5 mm but only one third as deep as those in Figure 1(c) could be detected. However, at 2 mm distance only images similar to Figure 1(a) were recorded.

In the preparative run with ground materials, product isolation shows conversion into triphenylacetophenone (**3**). There can be no doubt that the features formed in

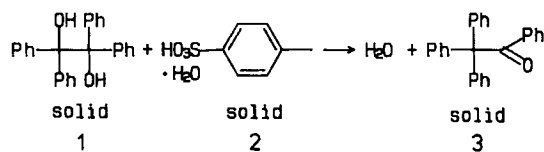


Figure 1 are the result of the 'pinacol rearrangement' ([1, 2, 3]-elimination of water).³ The water of reaction is released into the gas phase and if it is condensed out a dramatic increase in reaction rate and a 100% yield are observed.

The anisotropies and well directed molecular transports require an interpretation on the basis of x-ray structural data. The crystal structure of the pinacol **1**⁵ indicates infinite ribbons of hydrogen bonded molecules. In Figure 2 (and Figure 5) are depicted only one sort of disordered molecules. Polar 'channels' of OH-OH bridges though interrupted by C-1 and C-2 are seen. They run parallel to (100) or (001) in the [010]-direction. The differences in these faces are clearly seen in the three-dimensional wire diagrams in Figure 2. Thus, on the reactive (100) face the long axis of the molecules lies roughly in the surface plane along [001] with one phenyl group of each benzhydryl-C of the pinacol **1** pointing out of the face with interplanar

angles of 42.5° and 79° (Figure 2). On the other hand, on the non-reactive (001) face the long molecular axis is roughly perpendicular to the surface plane (again along [001]) with both phenyl groups of only one benzhydryl-C of **1** pointing out of that face at angles of 33° and 54°. According to Figure 3, the space demand within the layers of flatly lying molecules is not so large as in the case of the steeply standing molecules in Figure 4.

While this reasoning might be helpful in realizing the difference in reactivity on the different faces, it should also be realized that much more space demanding processes have been found already in other reactions of crystals and successfully handled with the new principle of phase rebuilding (see Refs 2, 4 and 6; this culminates in solid-state *cis-trans* isomerizations⁷). Therefore, more direct explanations of face-selective reactivities are required and these are found in the detailed shape of the crystal surfaces.

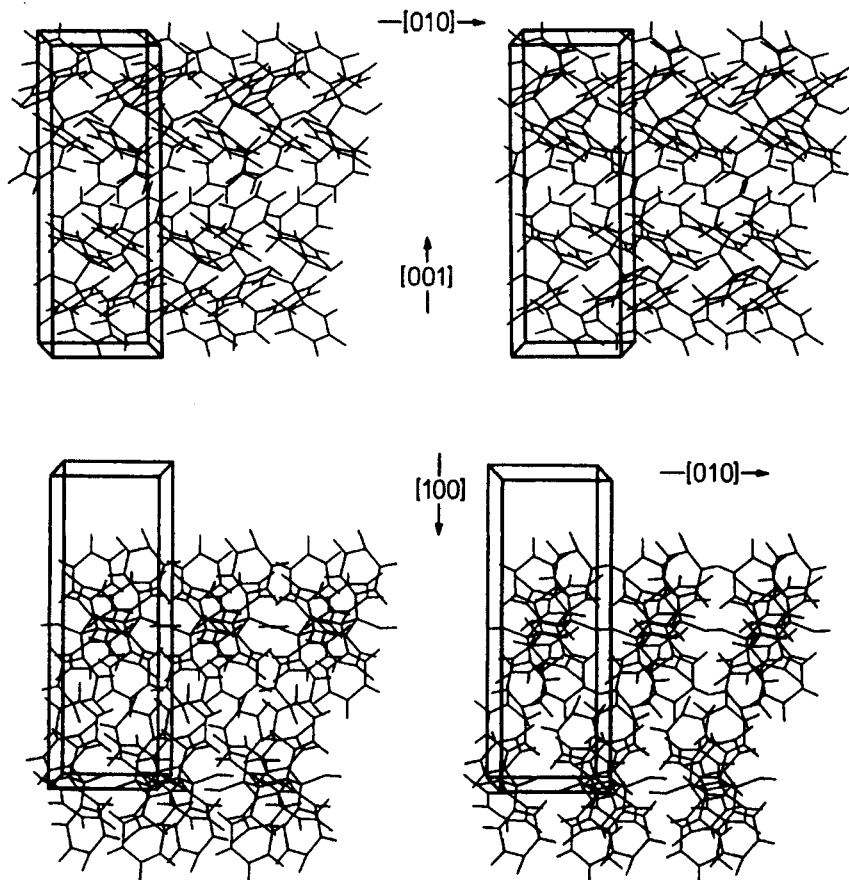


Figure 2. Stereoscopic wire model of the molecular packing of **1** showing 11 molecules. Top, view on the reactive face (100); bottom, view on the non-reactive face (001)

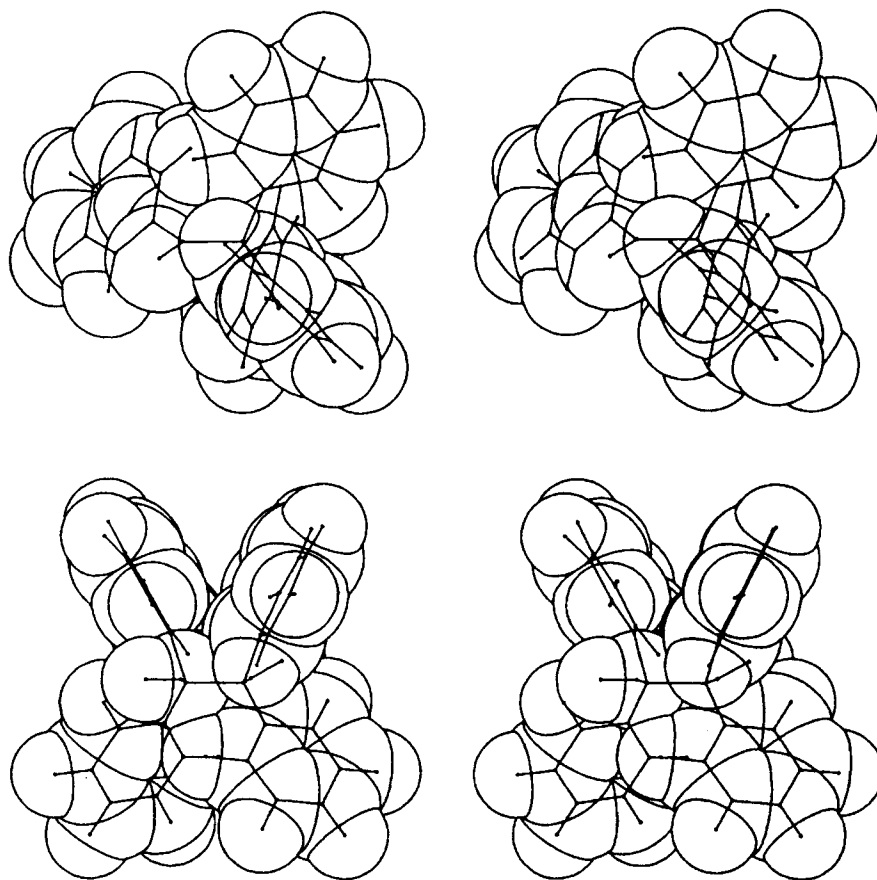


Figure 3. Space-filling transparent stereorepresentation of molecular shapes showing the flat-lying type of orientation as in the layers of the crystals of **1** under its reactive surface (100). Top, **3**, PM3 data; bottom, **1**, x-ray data for the H-bridged geometry⁵

Figure 5 shows space-filling surface models. It is seen that the phenyl groups which are pointing out of the surfaces are effectively shielding the polar groups in both cases; however, closer inspection of the stereodrawings reveals important differences. For a reaction of diol **1** to occur, a catalytic proton has to be attached to one of the OH groups. As can be seen from Figure 5, this will be virtually impossible on (001) because the oxygen atoms are extremely shielded and the hydrogens bound to them are pointing outwards. Thus, a proton from the contacting solid acid **2** may not approach and start the reaction on (001). However, on (100) the shielding may be less efficient, even though the phenyl groups stand steeper (see above), and the hydrogens attached to the oxygen atoms are underneath or on the same level. Therefore, protonation is possible on (100) and the reaction can start.

For the lateral and vertical spreading of the reaction up to 1.5 mm and at least 20 nm catalytic quantities of

protons have to move along the polar 'channels' but also between them while producing some charge separation. The shortest distances between an O-bound H from one side of the molecule to the other side are 4.290 and 4.550 Å. The shortest distances between the 'channels' are 8.524 Å in [001] and 9.134 Å in the [100] direction. As the proton regenerates on the other side of the molecule **1** to where the water is formed with an elimination rearrangement, it can attack the next molecule of **1** and enforce the reaction further and further away, leaving behind the water formed and the solid proton source with the counterion. This is most easily comprehended within the polar 'channel'. However, for the concentric and vertical spreading (i.e. perpendicular to the [010] direction), interchannel movement of the proton is required. This event needs the opening of links to the neighbouring polar 'channels' which should be facilitated by the phase rebuilding^{2,6} which is manifest in the features formed in Figure 1. Thus, the

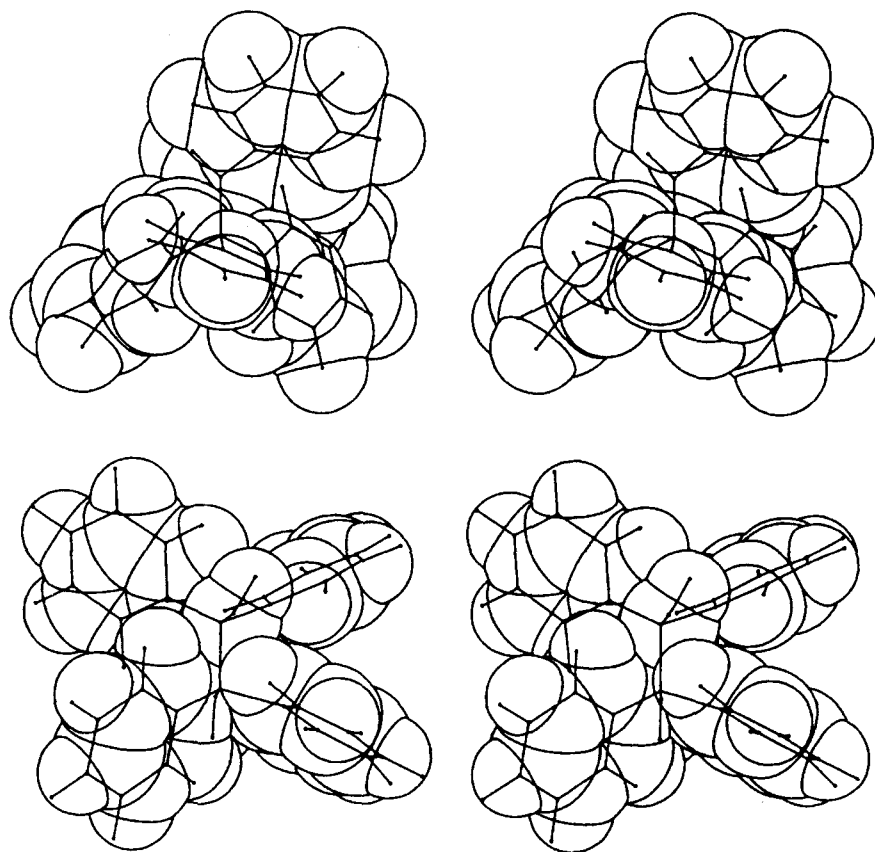


Figure 4. Space-filling transparent stereorepresentation of molecular shapes showing the steeply standing type of orientation as in the layers of the crystals of **1** under its non-reactive surface (001). Top, **3**, PM3 data; bottom, **1**, x-ray data for the H-bridged geometry⁵

product molecules **3** will initially have to accommodate the lattice of **1** and in doing so they will make the necessary turns, moves and molecular transports which lead to the features of Figure 1. Only at high conversions (very close to the edge) might a switch to the lattice of product **3** have occurred. Upward transport while leaving craters [Figure 1(c) and (d)] is a frequently observed phase rebuilding mechanism.^{2,6,8}

The crystal-crystal reaction found clearly leads to interesting proton migrations via continuous consumption and spatially distant reproduction over the remarkably large distance of 1.5 mm. Only a few catalytic protons will do the job because the anions left behind cannot build up to a high concentration at the site of the solid **2**. There appears to be no concomitant movement of anions over the surface: the solid proton source **2** adheres firmly to the initial crystal of diol **1**. On breaking it off, a very sharp borderline is seen, but no spreading to any side.

Although we cannot assess the depth of reaction underneath the solid catalyst, it is seen that beside it only a few molecular layers have reacted at 0.1, 0.5 and 1 mm lateral distances. Thus, for preparative runs the process requires over-stoichiometric amounts of solid acid **2** and grinding of the materials. However, under these conditions the front ends of the polar 'channels' will also be accessible. The 'channels' are precisely perpendicular under (010), a face which does not naturally occur on our single crystals [the skew (110) face under which the polar 'channels' run diagonal could not be measured with the AFM]. It will be easiest to inject protons into such surfaces (no steric hindrance); however, the charge separation limits their number, again for energetic reasons. Finally, it should be pointed out that AFM does not indicate the compound ratio **1**:**3** on the various features in Figure 1. However, good prospects exist for the settlement of such questions when scanning near-field optical micro-

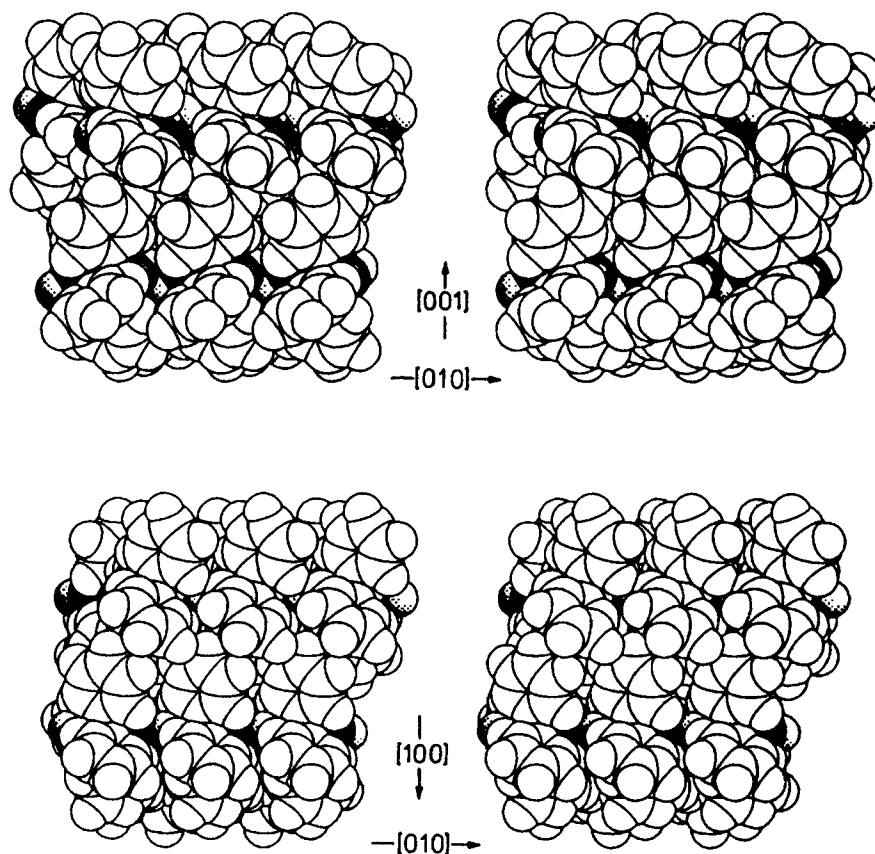


Figure 5. Space-filling stereorepresentation of the crystal surfaces of **1** showing the hydrogen bridging and the shielding of the polar groups by the phenyl residues. Top, view of the reactive (100) face; bottom, view of the non-reactive (001) face (black circles, O; dotted circles, O-bound H)

scopes with high dynamics in the Z-direction become commercially available.⁹ As no side products are formed in the preparative runs, chemical change in the surface region must not differ from giving water and rearranged product **3**. There is no reasonable basis to assume a different chemical process only at the surface.

CONCLUSIONS

The experimental data presented here are the result of the first AFM investigation of a solid–solid reaction. They show that unprecedented molecular mechanisms can be derived although the formation of surface features is similar to gas–solid reactions^{2,6} or to solid-state photoreactions.^{6,7} Charge separation by consuming catalytic protons and releasing new ones in separated compartments is obvious. That mechanism is clearly

indicated by the crystal structure. Reactivity or non-reactivity is determined by the up or down orientation of the O-bound hydrogens in the uppermost layer. These mechanistic views are strongly supported by the fact that the reacting crystals of **2** adhere firmly to the reactive (100) surface of the pinacol **1**, whereas contacting crystals of acid **2** do not adhere to the non-reactive (001) surface of pinacol **1** after 12 h of heating at 50 °C. Equally precise mechanistic details are expected from probing other types of solid–solid reactions with the AFM. Clearly, we now have a good basis to proceed with ionic, non-ionic and non-catalytic solid–solid reactions which run on a preparative scale.¹ This endeavour is of major importance because virtually nothing is known yet about the mechanisms of organic solid–solid reactions and these will have to be put on a reasonable extrapolation basis for further development in the field of future reaction techniques.

EXPERIMENTAL

The pinacol rearrangement was performed on a preparative scale by mixing **1** (3.66 g, 10 mmol, m.p. 186 °C) and **2** (5.71 g, 30 mmol, m.p. 106 °C). After grinding in a mortar, the mixture was heated in a flask under vacuum at 50 °C for 1 h. The water of reaction was condensed out in a second flask, which was connected to the reaction flask on a vacuum line and cooled to 77 K. After thorough washings of the reaction mixture with excess 2 M NaOH to remove all acid, a quantitative yield of pure **3** (m.p. 184 °C) was found but no tetraphenylloxirane.¹⁰ If the water of reaction was not condensed out, the reaction mixture remained solid for 24 h, because at least 1.7% (by weight) of water can be taken up by crystalline **2** at 50 °C without liquefying (TGA; after uptake of 3.5% water, **2** becomes partly liquid). However, the yield dropped to only 42% at 24 h, when the water of reaction was not efficiently removed. Strong peaks of **2** in the IR regions of interest prevented direct IR analysis. In this run the acid-free product mixture was analysed by HPLC [RP-18 column; elution with CH₃OH–H₂O (80:20, v/v)] and the product isolated by column chromatography on neutral silica (silica gel S, 0.063–0.10 mm; Riedel–de Haën) with toluene–cyclohexane (1:1, v/v). The first fraction was **3** (1.46 g, 42%) and the second unchanged **1** (1.98 g, 54%).

For AFM techniques, see Refs 2, 4, 6 and 8.

Thermogravimetric analyses (TGA) were carried out with a Perkin-Elmer TGA 7 instrument at 20 °C min⁻¹.

Crystals of *p*-toluenesulphonic acid monohydrate **2** (99%, Aldrich) were dried for 12 h at room temperature under vacuum and had the theoretical composition after that treatment, according to TGA. They were slightly hygroscopic and assumed a weight increase of 0.3% on TGA measurements when kept at 75 °C in air of 60% ambient relative humidity.

A tiny crystal (about 1 mm) of **2** was laid down on the fresh surface of a single crystal of **1** (about 8 mm wide, grown from benzene–cyclohexane by slow evaporation), which was previously mounted on a sticky conductive tab (Plano) on the AFM support (iron disc) with the desired crystallographic face on top. AFM scans were taken at distances of about 2, 1, 0.5 and 0.1 mm from the edge of contact of the two crystals, as judged by microscopic inspection. The AFM scans were repeated at various time intervals. The experiments at 50 °C under vacuum were performed by removing the whole support with the sample immediately after the initial measurements and placing it on a flat, tightly covered tray, which was heated at 50.0 °C for 2–12 h.

Thereafter the support was mounted on the AFM and measurements were undertaken as close as possible to the original sites in the ambient atmosphere. The crystal of **2** firmly adhering to that of **1** on (100) after 12 h at 50 °C could be broken off by applying manual force using tweezers, thus leaving a shallow glassy surface at the previous contact region with a very sharp borderline, as judged microscopically at 100-fold magnification. On the other hand, crystals of **2** on (001) of diol **1** did not adhere and fell on turning the larger crystal without leaving observable traces of interaction. PM3 calculations according to Stewart¹¹ with Spartan version 2.0 from Wavefunction (Irvine, CA, USA) and crystal or molecule modelling with Schakal 92 (E. Keller, Universität Freiburg, Germany) were performed on an IBM RS 6000 32H AIX-UNIX Workstation.

ACKNOWLEDGEMENTS

We thank Dr R. Boese, Universität Essen, for the determination of the Miller indices of the crystals of **1**. This paper is dedicated to Professor Hans-Jürgen Bestmann on the occasion of his 70th birthday.

REFERENCES

1. F. Toda, in *Reactivity in Molecular Crystals*, edited by Y. Ohashi, pp. 177–201. Kodansha, Tokyo, and VCH, Weinheim (1993).
2. G. Kaupp, *Mol. Cryst. Liq. Cryst.* **242**, 153–169 (1994); G. Kaupp and J. Schmeyer, *Angew. Chem., Int. Ed. Engl.* **32**, 1587–1589 (1993).
3. Selectivities: F. Toda and T. Shigemasa, *J. Chem. Soc., Perkin Trans. 1* 209–211 (1989); for the classification of the 'pinacol rearrangement' as [1,2,3]-elimination of water (with rearrangement as indicated), see G. Kaupp, *Top. Curr. Chem.* **146**, 57–98 (1988).
4. G. Kaupp, *J. Vac. Sci. Technol. B* **12**, 1952–1956 (1994); *Mol. Cryst. Liq. Cryst.* **252**, 259–268 (1994).
5. D. R. Bond, S. A. Bourne, L. R. Nassimbeni and F. Toda, *J. Cryst. Spectrosc. Res.* **19**, 809–822 (1989).
6. G. Kaupp, *GIT Fachz. Labor* **37**, 284–294 and 581–586 (1993) (English translations are available from the author); G. Kaupp and M. Plagmann, *J. Photochem. Photobiol. A: Chem.* **80**, 399–407 (1994).
7. Review: G. Kaupp, *Adv. Photochem.* **19**, 119–177 (1994).
8. G. Kaupp, *J. Microsc.* **174**, 15–22 (1994); *Mol. Cryst. Liq. Cryst.* **211**, 1–15 (1992); *Angew. Chem., Int. Ed. Engl.* **31**, 592–595 and 595–598 (1992).
9. E. Betzig, P. L. Finn and J. S. Weiner, *Appl. Phys. Lett.* **60**, 2484–2486 (1992).
10. H. J. Gebhart and K. H. Adams, *J. Am. Chem. Soc.* **76**, 3925–3930 (1954).
11. J. J. P. Stewart, *J. Comput. Chem.* **10**, 209–220 (1989).